



Spin-birefringence in molecular currents: Tellurium and gold complexes

Amlan K. Roy^a, Joseph L. Speyer^b, Lizette Bartell^b, Daniel Neuhauser^{b,*}

^a IISER, Division of Chemical Sciences, Mohanpur Campus, Nadia, WB 741252, India

^b Department of Chemistry and Biochemistry, University of California, Los Angeles, CA 90095-1569, United States

ARTICLE INFO

Article history:

Received 5 September 2009

In final form 1 December 2009

Available online 4 December 2009

ABSTRACT

We simulate the spin-flip current and transmission function through rings containing elements with a spin-orbit interaction. In a previous study (J. Chem. Phys. 123 (2005) 204714) we predicted that such a system can show spin-birefringence, i.e., a spin current polarized parallel to the molecular axis can flip its direction due to a phase lag due to the spin-orbit interaction. Here we demonstrate the effect in a semi-empirical extended Hückel theory (EHT) molecular simulation. The ring systems studied are naphthalene-bitellurium, gold-porphyrin, and cyclometallated chlorogold, connected to polyacetylene.

© 2009 Published by Elsevier B.V.

1. Introduction

A rapidly emerging field in modern microelectronics is spintronics [1,2], the use of electron spin degrees of freedom to process, store and transmit information, in contrast to semiconductor electronics where this role is played by the charge. Spintronics discoveries include giant magnetoresistance and the spin-valve effect in metallic multilayers, and spintronics may eventually be crucial for quantum computation.

It is natural to ask whether spin-dependent transport can be accomplished in molecular electronics. Although such a combination has been mostly studied in the context of inorganic semiconductors [3,4], the possible use of other materials in spintronics, e.g., π conjugated semiconductor, organometallic, molecular wire, and atomic carbon wire, DNA molecular monolayer and carbon nanotubes [5–10], has also been explored considerably in the past few years, leading to molecular spintronics. Recently, the use of spin-polarized graphene has also attracted much attention [11].

The manipulation of the spin-polarized current can be done by magnetic fields (responsible for the Zeeman and Aharonov–Bohm effects); this however is potentially difficult since the direct effect of the magnetic fields on the electrons is proportional to the area on which they act, making their effect small for nano and sub-nano systems unless very large fields are used.

Recently it was proposed [12] that spin-orbit coupling could also be exploited to influence spintronics in ring-type devices which contain one or a few atoms with strong spin-orbit interaction. By coupling the ring to a lead at an angle the $l_z \rightarrow -l_z$ symmetry of the loop can be broken, i.e., the coupling of the ring states to incoming and outgoing states is asymmetrical.

The asymmetric coupling leads to an interesting birefringence phenomena in which there is a phase lag between the different conserved 'z' polarizations of a planar device. Birefringence implies that if the spin is initially polarized in, e.g., the 'x' direction, i.e., is the coherent sum of the two 'z' polarizations, then as a function of initial energy it can come out polarized in the 'x' direction or be polarized in the opposite direction, '-x', depending on the phase lag between the two 'z' polarizations. In short, a molecule can flip the spin.

Here we move beyond the schematic model systems in Ref. [12] to a more explicit molecular simulation with atoms that have strong spin-orbit coupling. The first system is a tellurium dimer connected to a ring-like structure, in our case naphthalene. This creates an effective triangle with the spin-orbit atom in one vertex. The other two vertices are then coupled at an angle to two polyacetylene wires.

The second type of compounds contains gold. We examine first the connection of gold to a porphyrin group. In addition, we study chlorogold, a gold atom complexed to a chlorine atom and connected to a pyridine ring and two benzene rings, forming a triangular structure again. In this case the compounds are again coupled at an angle to two polyacetylene wires. The presence of the non-linear angle is important to produce an effect mimicking that of the original model system, where the shift away from the linear angle broke the $l_z \rightarrow -l_z$ symmetry.

The atomic model is studied here with a fairly quantitative approach, extended Hückel theory (EHT) [13], using the Landauer–Büttiker formalism with a non-equilibrium Green's function methods (see e.g., [5,8,14,15]), based here on the use of absorbing potentials. EHT can handle large systems and describes the relevant excitation energies well.

Section 2 gives details of the wire-loop geometry. Section 3 describes the EHT method used to construct the Hamiltonian corresponding to the extended system; spin-orbit interaction is

* Corresponding author.

E-mail address: dxn@chem.ucla.edu (D. Neuhauser).

included in the Hamiltonian locally. The transmission probability functions as well as the current–voltage features are calculated using a Green’s function formalism. Section 4 presents the results and conclusions follow in Section 5.

2. Systems studied

The three molecular systems studied are shown in Fig. 1. Current flows through a linear planar *trans* polyacetylene chain (not shown), which acts as a ‘lead’. The molecular loop is sandwiched between two leads (having 44 –CH– groups each) connected at an angle. The loop in (a) consists of a π conjugated naphthalene aromatic ring disubstituted at the 1 and 8 positions with two Te atoms, which are covalently bonded to each other again in the same plain. This geometry was inspired by the recent use of a closely related Te based compound *periditellurium*-bridged polyacene donor complex, 2,3,6,7-tetramethylnaphtho[1,8-*cd*:4,5-*c’d'*]bis[1,2]ditellurole (TMTTeN) in molecular electronics applications [16]. The other geometries studied are (b) a porphyrinato gold complex [17] and (c) a cyclometallated chlorogold(III) complex [18]. All ground-state geometries were obtained by GAUSSIAN03 [19] using RHF/STO-3G.

3. Methodology

3.1. EHT

Several analogues of tight-binding semi-empirical methods have been suggested for studying molecular conductance and electron transfer. We use EHT, and the EHT Hamiltonians were generated using ICoN-Edit [20]. EHT Hamiltonians have been used extensively in electronics simulations [21,22], and have also been used specifically for molecular conduction [23]. The advantages of EHT are its low number of parameters, its modest computational expense, and its transferability. In addition, EHT has compared favorably with density functional theory in predicting band gaps as well as changes in electronic structure [21].

While the charge distribution is not calculated in a self-consistent manner here, the overall effect of spin-birefringence is not dependent on the specific form of the charge distribution, as will be shown later. The transport itself is not expected to influence the molecular geometries and energy levels much; rather, the voltage difference will shift the energy level, but as shown later the results are not qualitatively sensitive to these effects.

The EHT Hamiltonian, H_0 , solves

$$H_0 C = S C \varepsilon, \quad (1)$$

where C is the coefficient matrix and S is the overlap matrix.

The basis functions used here are not orthonormal, and need to be orthogonalized, by defining

$$C' = S^{1/2} C, \quad (2)$$

so

$$H C' = C' \varepsilon, \quad (3)$$

where

$$H = S^{-1/2} H_0 S^{-1/2}. \quad (4)$$

The Hamiltonian is supplemented by absorbing potentials on each lead, Γ_L and Γ_R , so that the Green’s function for the interacting system is [24]

$$G(E) = \frac{1}{(E - H + i\Gamma_L + i\Gamma_R)}. \quad (5)$$

One interesting question is whether the absorbing matrices Γ_L and Γ_R need to be likewise rotated via $S^{-1/2}$, i.e., whether Γ_L and Γ_R should be diagonal matrices (each non-zero only near the ends of the left or the right lead) or should they be rotated to be $S^{-1/2} \Gamma_{L0} S^{-1/2}$ (and similarly for Γ_R), where Γ_{L0} is a diagonal matrix. Luckily, the effect of rotating the absorbing matrices was found to be negligible, as shown later, so that either choice is acceptable.

3.2. Spin-orbit

The EHT Hamiltonian is supplemented by a spin-orbit term, which is taken to be $\eta \vec{L} \cdot \vec{S}$, where η is an atom-dependent constant which depends on the element involved. For Te, this value is 3384 cm^{-1} from the HF wave functions. For Au, this value is 5104 cm^{-1} from the HF wave functions [25]. Note that the spin-orbit term is localized on each atom. Physically, the reason is that the spin-orbit term is generated due to motion of core electrons and is a rapidly falling function of the distance from the nucleus of the heavy atom; therefore, it is reasonable to assume that it needs to be considered only over the valence orbital of the heavy atoms.

Further, since the basis set is not completely orthonormal, there is uncertainty over whether a local description is completely quantitative; however, in practice, the inaccuracies this introduces are small. Thus, we got very similar results (Fig. 9b) if we add $\eta \vec{L} \cdot \vec{S}$ to H_0 or H .

The electron transmission probability from source to drain across the molecular wire for small bias is calculated by the flux–flux formula [26].

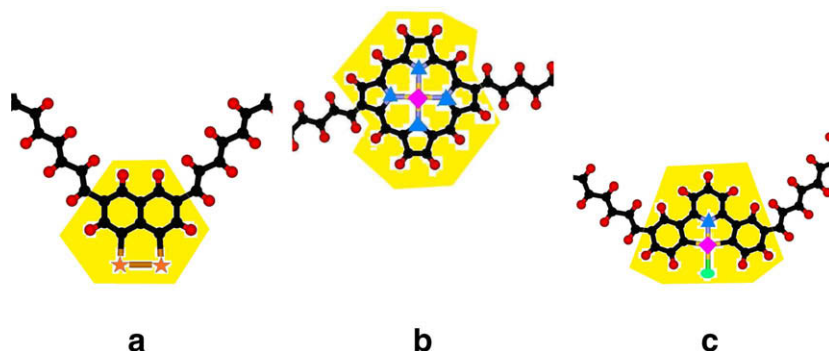


Fig. 1. Ground-state optimized geometries of the molecular wires. Orange stars denote Te, magenta diamonds denote Au, blue triangles denote N, green ovals denote Cl, black circles denote C and red circles denote H. The shaded regions are the molecular loops. The polyacetylene leads connected to each complex are not fully displayed. Above, the molecules are (a) a naphthalene-bitellurium complex; (b) a gold-porphyrin complex; and (c) a cyclometallated chlorogold complex. (For interpretation of the references in colour in this figure legend, the reader is referred to the web version of this article.)

$$N(E) = 4 \text{Tr}(\Gamma_L G(E) \Gamma_R G^\dagger(E)). \quad (6)$$

We generally used absorbing potentials of length 20 Å with maximum peak at 10.0 eV. These parameters were found to be appropriate to achieve convergence.

Current is calculated using the Landauer–Büttiker equation in the limit of zero temperature [27],

$$I(V) = \frac{2e}{h} \int_{E_f - V/2}^{E_f + V/2} N(E) dE. \quad (7)$$

Here, E_f is the Fermi energy. The spacers and leads considered here are polyacetylene, which has a band-gap due to Peierls bond-alternation. In reality, the true leads will have to be a metal (e.g., gold, or even doped polyacetylene) or a narrow-band semiconductor; we did not simulate this part of the leads, but simply assumed the device will be gated so that the Fermi energy of the true leads will match the HOMO of the polyacetylene, at -11.67 eV for the EHT calculations, so that we consider here hole conduction. Since the band gap of the polyacetylene is smaller than that of the inherent molecular system, the non-metallicity of the leads does not affect quantitatively the results, as shown below.

Another potentially important aspect is the charge distribution. Since the spin-orbit effect is local, the results are not expected to depend on the specific voltage distribution in the molecule. Therefore, in most simulations we assume that the voltage on the molecule is constant. To confirm that this assumption is immaterial we have done an additional set of simulations in which there is a linear voltage drop off along the molecule. As will be shown later, the results are qualitatively similar for different voltage distributions assumed along the molecule.

Finally, the main part of the calculations is the computation of the flip transmission, defined as the summed probability to start with an up spin along the x -axis and end up with a down spin (by symmetry it can be shown that this is the same as the probability to start with down spin and end up with up spin, as we also verified numerically). This summed probability is calculated as,

$$N_{\text{flip}}(E) = 4 \text{Tr}(\Gamma_L P_+ G(E) \Gamma_R P_- G^\dagger(E)), \quad (8)$$

where P_\pm are projection operators to a spin polarized in the positive and negative x -axis (the long axis of the polymer) defined as

$$P_+ = (|\alpha\rangle + |\beta\rangle)(\langle\alpha| + \langle\beta|)/2, \quad (9)$$

and similarly for P_- ; $|\alpha\rangle$ and $|\beta\rangle$ denote the semi-conserved spin components along z , the axis perpendicular to the molecule.

4. Results and discussion

Figs. 2 and 3 display the electron transmission across the molecular wire as function of energies (in eV) for the three molecular wire-loops shown in Fig. 1a–c; Fig. 2 is for flip transmission and Fig. 3 for non-flip transmission. The spin-dependent transmission for ditellurium is not very high, especially near the Fermi energy. The same is true for gold–porphyrin, but the results for chlorogold are more promising. Importantly, this is also true near the Fermi energy of -11.75 eV. Note that the Fermi energy (-11.67 eV in the polyacetylene wire EHT calculation) is too low compared with more accurate RHF and DFT calculations, which predict it at between -6 and -5 eV; therefore, in principle all energies should be shifted upward by the difference in free energies, about 6 eV, and should therefore not be interpreted literally. This shift is not done in the figures below since it does not impact the main conclusions, i.e., the I vs. V curves. Figs. 4 and 5 display the corresponding current–voltage graphs.

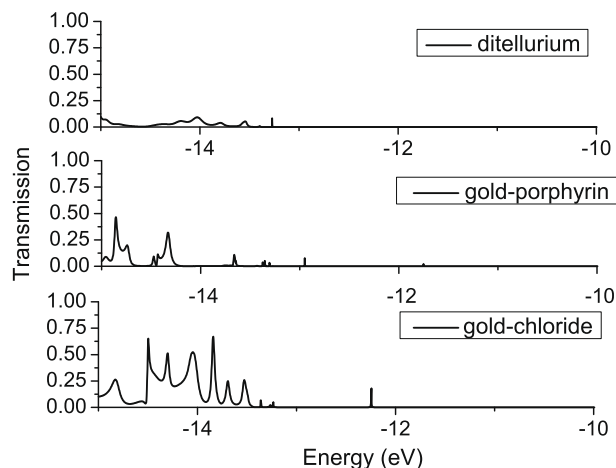


Fig. 2. Flip electron transmission ($N(E)$) as a function of energy for the ditellurium, gold–porphyrin and chlorogold complexes. The above show the ditellurium as having little electron transmission, but it is more significant for the gold–porphyrin, with even higher electron transmission for the chlorogold complex.

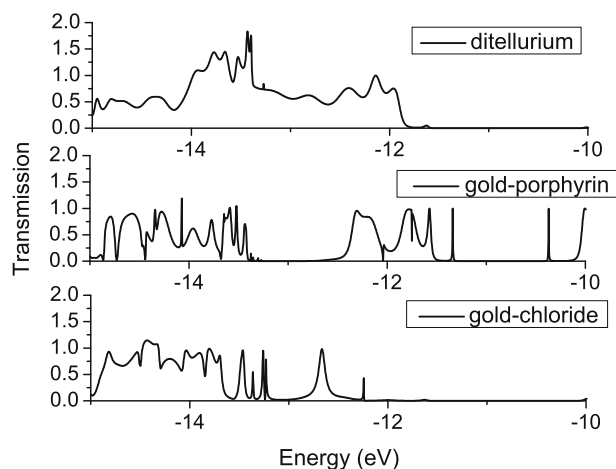


Fig. 3. Non-flip electron transmission ($N(E)$) as a function of energy for the ditellurium, gold–porphyrin and chlorogold complexes. The above graphs show the electron transmission decreasing from the ditellurium to the chlorogold complex. This is consistent with the results for the flip electron transmission.

As the results from chlorogold were promising (Fig. 6), they were followed by a study of two chlorogold functional regions in tandem (Fig. 7) with all other factors remaining unchanged. Fig. 8 clearly shows that using two chlorogold groups in tandem dramatically improves the ratio of spin-flip to total conduction.

To verify that the absorbing potentials can be used properly within the EHT formalism, we simulated (Fig. 9) the flip transmission for the chlorogold molecule with both rotated and unrotated absorbing potentials (i.e., adding to H either $S^{-1/2}(\Gamma_L + \Gamma_R)S^{-1/2}$ or $(\Gamma_L + \Gamma_R)$). The results are identical, proving that there is no ambiguity in the application of the absorbing potentials in EHT.

Finally, we studied two important methodological aspects mentioned above. First, the dependence on the specific leads used. As mentioned, polyacetylene has bond alternation, and therefore a band gap of order 1.5–2 eV; to verify that this band gap is immaterial to the results we simulated the chlorogold molecule again, now using idealized leads with polyacetylene with equally spaced bonds. Such idealized leads are metallic. As Fig. 10 shows, this does not impact the results significantly; both idealized and alternating leads give the same results. The reason is clear – the birefringence

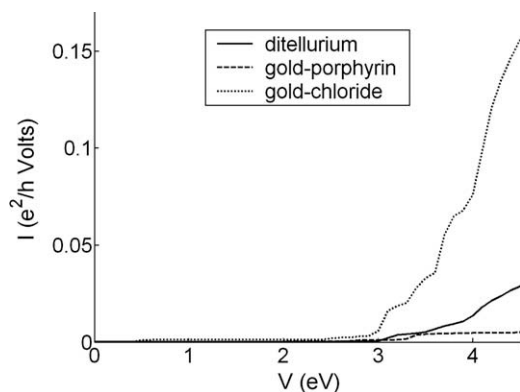


Fig. 4. Flip current as a function of voltage for the ditellurium, gold-porphyrin and chlorogold compounds. The graphs show an increase in flip current at higher voltages, i.e., as one moves away from the Fermi energy.

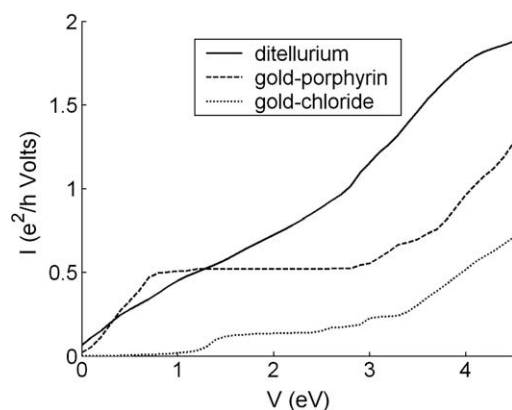


Fig. 5. Non-flip current as a function of voltage for the ditellurium, gold-porphyrin and chlorogold compounds. An increase in voltage raises immediately the non-flip current, since the non-flip transmission is significant even near the Fermi energy.

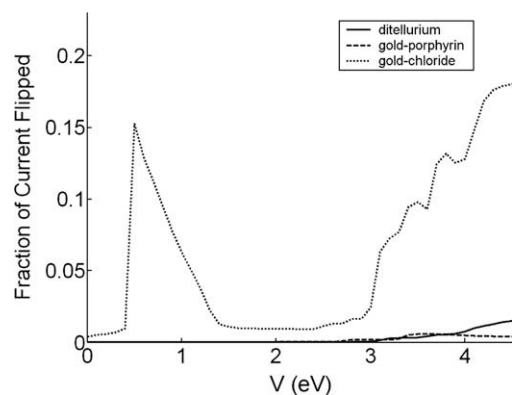


Fig. 6. Flip current as a fraction of total current for ditellurium, gold-porphyrin and chlorogold compounds. Chlorogold shows significant current flip ratio both at low voltages (near 1 V) where both currents are very small, and, more importantly, at higher currents (above 3 V) where $V/2$ approaches the band gap around 1.5–2 V.

effect is local (due to the spin-orbit) and involves interference within the actual molecule, and the nature of the leads is not important for this qualitative effect.

In addition, simulations were performed to ensure that the form in which the voltage was applied to the molecule did not affect the overall results. A voltage was applied in four different ways: as a flat voltage applied across the entire molecule, as a flat voltage

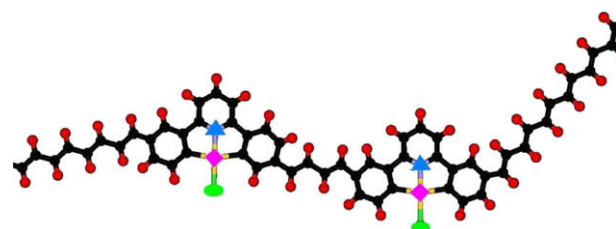


Fig. 7. Optimized ground-state, obtained by using RHF/STO3G, of the chlorogold groups in tandem, as well as the molecular wire. Magenta diamonds denote Au, blue triangles denote N, green ovals denote Cl, black circles denote C and red circles denote H. The polyacetylene leads are not fully displayed. (For interpretation of the references in colour in this figure legend, the reader is referred to the web version of this article.)

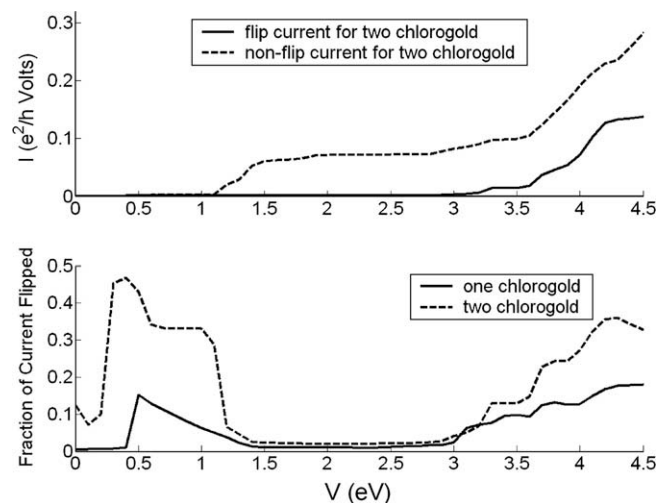


Fig. 8. (top) Flip and non-flip current as a function of voltage for molecule with two chlorogold rings. (bottom) Flip current as a fraction of total current for a molecule with one (solid line) and two (dashed line) chlorogold rings. The graph shows a significant increase in flipped current using the molecule with the two chlorogold rings in tandem.

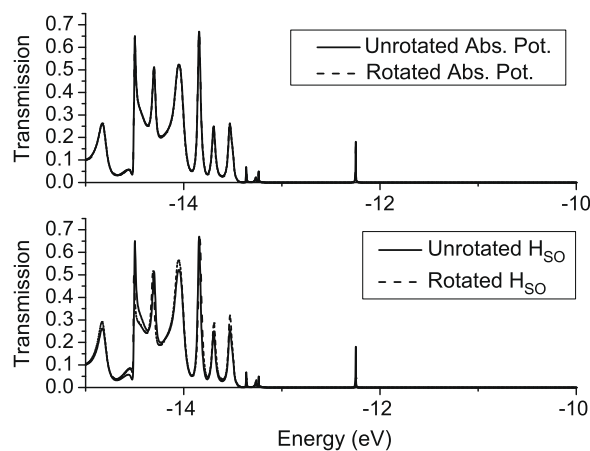


Fig. 9. (top) Flip transmission ($N(E)$) as a function of energy for the chlorogold molecule with both rotated and unrotated absorbing potentials. (bottom) Flip transmission ($N(E)$) as a function of energy for the chlorogold molecule with both rotated and unrotated H_{SO} . In both cases, the two curves are virtually indistinguishable.

with $V = -V/2$ on the incoming lead and $V = V/2$ on the outgoing lead and a linearly-varying voltage applied across the molecular loop, as a flat voltage with $V = -V/2$ on the incoming lead and

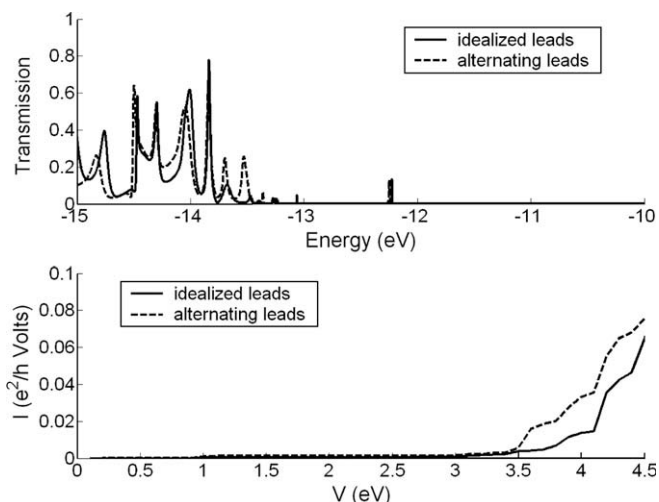


Fig. 10. (top) Flip electron transmission ($N(E)$) as a function of energy for the chlorogold complexes with idealized and alternating leads. (bottom) Flip electron current as a function of voltage for the chlorogold complexes with idealized and alternating leads. There are a few differences, but both types of leads produce similar flip electron transmissions.

$V = V/2$ on the outgoing lead and $V = 0$ on the molecular loop, and as a linear voltage ranging from $V = -V/2$ on the incoming lead to $V = V/2$ on the outgoing lead applied across the entire molecule. While applying a voltage directly on the molecule did alter $N(E)$, and thus $I(V)$, Fig. 11 shows that the spin-birefringence is not dependent on the specific voltage distribution used; both extremes, of a flat voltage along the molecule and a linearly-varying voltage distribution give similar results.

Note that all geometries were optimized at the Hartree–Fock (RHF/STO-3G) level and thus more detailed studies would be necessary to examine effects such as the suitability of basis set or use of density functional methods instead of EHT. A-priori, no physical effects are expected from a larger basis set. More accurate calculations are primarily expected to affect the charge distribution. The effects will be small relative to those expected from the fact that in the transport calculations, EHT is used with an assigned charge distribution as explained below, since EHT is not a self-consistent

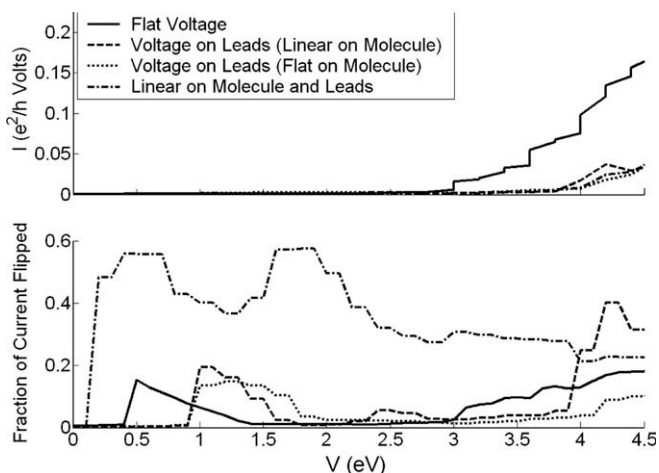


Fig. 11. (top) Flip current as a function of voltage for the molecule with one chlorogold ring, with a bias applied on the molecule in four different ways. (bottom) Flip current as a fraction of total current for the molecule with one chlorogold ring, with a bias applied on the molecule in four different ways.

polarizable method; however, as explained below, we find that the effects of different charge distributions are not qualitative, and therefore there is no need for highly accurate calculations. In addition the present work employs only a few model systems; many more remain uninvestigated.

5. Conclusions

In conclusion, we used here realistic simulations to demonstrate that spin-birefringence can be substantial in molecular systems and be controlled by the interactions of the molecular ring (naphthalene or other organic ring systems) and bounded heavy atoms (tellurium and gold here).

Note that all geometries were optimized at the RHF/STO-3G level and thus more detailed studies would be necessary to examine effects such as the suitability of basis set or use of density functional methods instead of EHT. In addition the present work employs only a few model systems; many more remain uninvestigated.

There are several interesting aspects to the study. First is the structure of the molecule; based on a simple birefringence picture, we could have predicted that the molecule itself, especially when two molecules are used in tandem, needs to be chiral rather than see-saw; however we found that a chiral combination (i.e., making the system spiral) is actually less effective in the spin-birefringence. This is a puzzling effect which needs to be further studied.

Another is the controllability. To be used as an actual device, two conditions must occur. First the incoming spin current must be polarized; this can presumably be achieved by connecting to a ferromagnetic lead. But equally important is the ability to gate this device. This can be done by brute force gating to prevent current passing through; a more interesting possibility is to keep the total transmission but to change the transmission characteristics from flip to non-flip and vice versa. This can be achieved in some systems by gating; we are working on the most interesting option, whereby rotating some chemical bonds can induce a change in the combination of the spin-orbit effect so that the spin-flip transmission will be changed.

Acknowledgments

We are grateful to Igor Ovchinnikov for useful discussions. This work is supported by the NSF.

Appendix A. Spin-orbit calculations

The first step in adding the spin-orbit coupling effect is to expand a spin-independent Hamiltonian into a spin-dependent Hamiltonian. The Hamiltonian is then considered to be the sum of the original Hamiltonian and a spin-orbit effect:

$$H = H_0 + H_{SO}, \quad (\text{A1})$$

where

$$H_{SO} = \eta \vec{L} \cdot \vec{S}, \quad (\text{A2})$$

and

$$\vec{L} \cdot \vec{S} = \frac{L_+ S_-}{2} + \frac{L_- S_+}{2} + L_z S_z, \quad (\text{A3})$$

so that, given a closed-shell EHT Hamiltonian using size N basis set $j = 1, 2, \dots, N$, of the form $|a_j, n_j, l_j, m_j\rangle$, where a, n, l, m denote the atom, principal quantum number, and the two angular indices), the full $2N \times 2N$ Hamiltonian is then:

$$\begin{aligned}
 H_{i\gamma,j\eta} = & (H_0)_{ij}\delta_{\gamma\eta} + \frac{\eta_{a_j}}{2} \langle l_i m_i | L_+ | l_j m_j \rangle \delta_{a_i a_j} (S_-)_{\gamma\eta} \\
 & + \frac{\eta_{a_j}}{2} \langle l_i m_i | L_- | l_j m_j \rangle \delta_{a_i a_j} (S_+)_{\gamma\eta} \\
 & + \eta_{a_j} \langle l_i m_i | L_z | l_j m_j \rangle \delta_{a_i a_j} (S_z)_{\gamma\eta},
 \end{aligned} \tag{A4}$$

where η_{a_j} is the spin-orbit amplitude for atom a_j .

References

- [1] I. Žutić, J. Fabian, S.D. Sarma, *Rev. Mod. Phys.* 76 (2004) 323.
- [2] M. Tanaka, *J. Cryst. Growth* 278 (2005) 25.
- [3] J.M. George, M. Elsen, V. Garcia, H. Jaffrès, R. Mattana, *C.R. Phys.* 6 (2005) 966.
- [4] H. Dalglish, G. Kirczenow, *Phys. Rev. B* 72 (2005) 155429.
- [5] E.G. Emberly, G. Kirczenow, *Chem. Phys.* 281 (2002) 311.
- [6] C.M. Schneider et al., *Diam. Relat. Mater.* 13 (2004) 215.
- [7] K. Tagami, M. Tsukada, *J. Phys. Chem. B* 108 (2004) 6441.
- [8] R. Liu, S.H. Ke, H.U. Baranger, W. Yang, *Nano Lett.* 5 (2005) 1959.
- [9] L. Senapati, R. Pati, M. Mailman, S.K. Nayak, *Phys. Rev. B* 72 (2005) 064416.
- [10] A.R. Rocha, V.M. García-Suárez, S.W. Bailey, C.J. Lambert, J. Ferrer, S. Sanvito, *Nature Mater.* 4 (2005) 335.
- [11] Y.W. Son, M.L. Cohen, *Nature* 444 (2006) 347.
- [12] I.V. Ovchinnikov, D. Neuhauser, *J. Chem. Phys.* 123 (2005) 204714.
- [13] R. Hoffmann, *J. Chem. Phys.* 39 (1963) 1397.
- [14] M. Zwolak, M.D. Ventra, *Appl. Phys. Lett.* 81 (2002) 925.
- [15] R. Pati, L. Senapati, P.M. Ajayan, S.K. Nayak, *Phys. Rev. B* 68 (2003) 100407(R).
- [16] E. Fujiwara, H. Fujiwara, et al., *Eur. J. Inorg. Chem.* 17 (2005) 3435.
- [17] M. Eng, T. Ljungdahl, J. Andréasson, J. Martensson, B. Albinsson, *J. Phys. Chem. A* 109 (2005) 1776.
- [18] K. Wong, K. Cheung, M. Chan, C. Che, *Organometallics* 17 (1998) 3505.
- [19] M.J. Frish et al., *GAUSSIAN 03*, Gaussian Inc., Pittsburgh, PA, 2003.
- [20] G. Calzaferrri, *QCPE Bull.* 92 (1993) 73.
- [21] D. Kienle, J.I. Cerda, A.W. Ghosh, *J. Appl. Phys.* 100 (2006) 043714.
- [22] P. Leyton, J.S. Gómez-Jeria, S. Sanchez-Cortes, C. Domingo, M. Campos-Vallette, *J. Phys. Chem. B* 110 (2006) 6470.
- [23] W. Tian, S. Datta, S. Hong, R. Reifenberger, J.I. Henderson, C.P. Kubiak, *J. Chem. Phys.* 109 (1998) 2874.
- [24] D. Neuhauser, M. Baer, *J. Chem. Phys.* 92 (1990) 3419.
- [25] S.L. Murov, I. Carmichael, G.L. Hug, *Handbook of Photochemistry*, Dekker, NY, 1993.
- [26] T. Seideman, W.H. Miller, *J. Chem. Phys.* 96 (1992) 4412.
- [27] S. Datta, *Electronic Transport in Mesoscopic Systems*, Cambridge University Press, 1995.